ANNALI DI GEOFISICA, VOL. 42, N. 2, April 1999

Improved compilation of Antarctic Peninsula magnetic data by new interactive grid suturing and blending methods

Ash Johnson ([1])(*), **Stephen Cheeseman** ([2]) **and Julie Ferris** ([1])
([1]) *British Antarctic Survey, High Cross, Cambridge, U.K.*
([2]) *Geosoft Inc., 8th Floor, 85 Richmond St W., Toronto, Canada*

Abstract
The utility of aeromagnetic and other geoscientific compilations on a range of scales, is well established for a wide variety of geological investigations. Aeromagnetic compilations, currently underway for the Antarctic continent are vital to take full advantage of existing aeromagnetic surveys and for planning new surveys of this relatively unknown continent. Grid compilation is often a time-consuming and subjective task, which requires considerable effort from the geoscientist involved. A new interactive grid compilation tool, GridKnit™, is presented, which enables the operator to rapidly combine gridded data sets with high quality results. The system offers two methods: a conventional blending method and a new suturing method. The blending method distributes the errors between grids over the area of overlap, effectively 'feathering' one grid into the other. The suturing method uses an analysis of the wavelengths of the data mismatches to correct each grid by an amount proportional to that wavelength. Each method has been applied to data sets from the Bellingshausen Sea-Alexander Island area of Antarctica to produce the first coherent magnetic map of this remote region.

Key words *aeromagnetic – grid compilation – GridKnit™*

1. Introduction

Compilations of magnetic data on scales from local to inter-continental have a range of uses, from delineation of local mineral exploration targets to supercontinent reconstructions. In recent years, an increasing number of continental-scale magnetic compilation projects have been undertaken, including the Antarctic Digital Magnetic Anomaly Project (ADMAP; Johnson *et al.*, 1997). Such compilations are powerful tools for determining the structure, geological processes and tectonic evolution of the continents.

Compiling magnetic data from widely varying sources, and with differing acquisition and processing parameters is necessarily a time-consuming task. The most rigorous methods involve re-processing original line data to uniform height, regional field removal and filtering. It is a fact, however, that many surveys, particularly (but not exclusively) older ones, often have little associated documentation, or may exist only as hardcopy contour or profile maps. Digital data may have been derived from such maps. In these cases, it is frequently impractical to re-reduce original profiles. An alternative to the profile-based method is to use

Mailing address: Dr. Ash Johnson, British Antarctic Survey, High Cross, Madingley Road, Cambridge, U.K.; e-mail: Ash.Johnson@Geosoft.com

(*) *Now at*: Geosoft Europe Ltd., 20/21 Market Place, Wallingford, OX10 0AD, U.K.

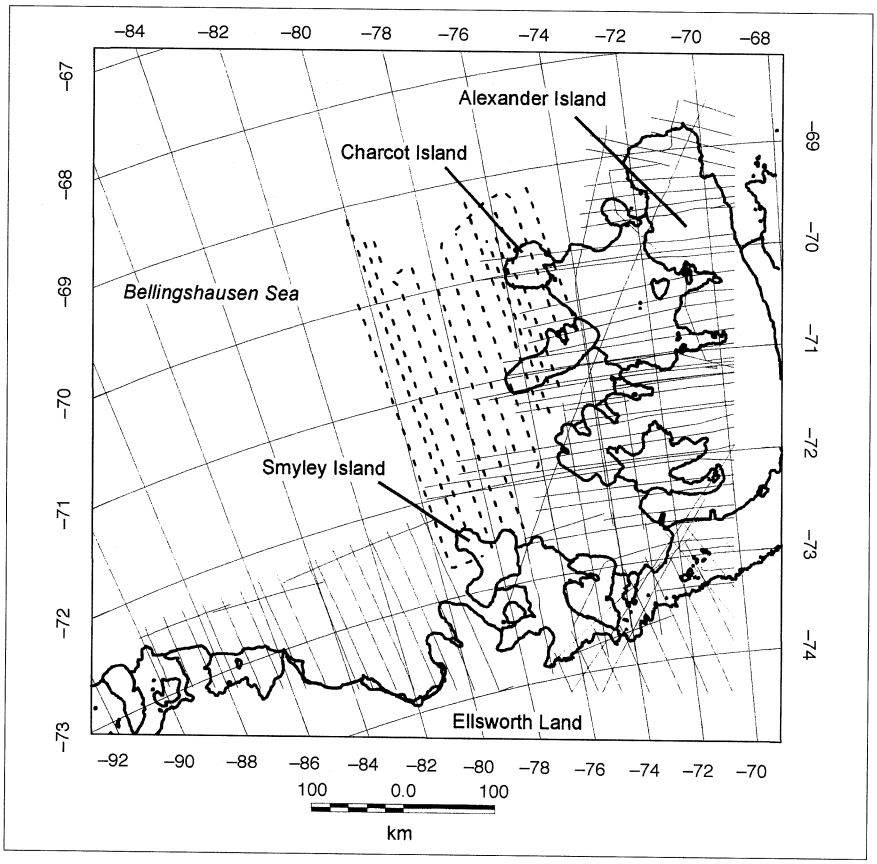

Fig. 1. Map of Alexander Island and Bellingshausen Sea area. Solid lines are reconnaissance aeromagnetic survey flight lines. Dashed lines are Charcot survey lines.

existing grid-based data. These can also be re-processed with consistent parameters if the necessary information exists, such as reference field and reduction height. Merging modern surveys with older data also gives rise to unique problems. It may not be desirable to re-process an internally consistent, processed and levelled modern data set alongside older, less accurate data. However, using the modern survey grid as a reference, and adjusting the older data may lead to a more acceptable final result.

Traditional grid-merging techniques include manual adjustment of grid edge values, levelling to existing low-resolution grids, or using various grid-weighting and smoothing algorithms (*e.g.*, Dods *et al.*, 1985; Fairhead *et al.*, 1997). All these methods are capable of producing smooth final products, but are time consuming and the validity of the final result may be questionable. Of particular concern is the loss of spectral integrity in the merged data set, which in turn may lead to erroneous further analysis and interpretation. In this paper, we demonstrate a new, rapid, interactive method developed to merge grids intelligently and seamlessly, using two different techniques. Each technique is applied to two magnetic grids from the Antarctic Peninsula of different age and quality, covering parts of the Bellingshausen Sea and Alexander Island (fig. 1).

2. Antarctic Peninsula data

British Antarctic Survey (BAS) reconnaissance aeromagnetic data covering much of the Antarctic Peninsula and Northern Ellsworth Land were acquired by the BAS between 1978 and 1987 (Renner *et al.*, 1985; Maslanyj *et al.*, 1991) using Twin Otter aircraft. Lines were flown at 20-50 km intervals, with widely spaced tie lines (fig. 1), at a height of 2500 m above mean sea level (m.s.l.). A wingtip-mounted proton precession magnetometer was used, with a measurement accuracy of 1 nT, and a passive magnetic compensation system. Navigation relied largely on Doppler methods, and can be regarded as accurate to 2 km (Renner *et al.*, 1985). Data were initially reduced to the 1980 International Geomagnetic Reference Field (IGRF; Barraclough, 1981), and subsequently re-reduced (Johnson and Smith, 1992) using the 1985 IGRF coefficients (Barraclough, 1985).

The aeromagnetic map derived from these data is shown in fig. 2, and the flight lines are shown in fig. 1. The band of positive anomalies

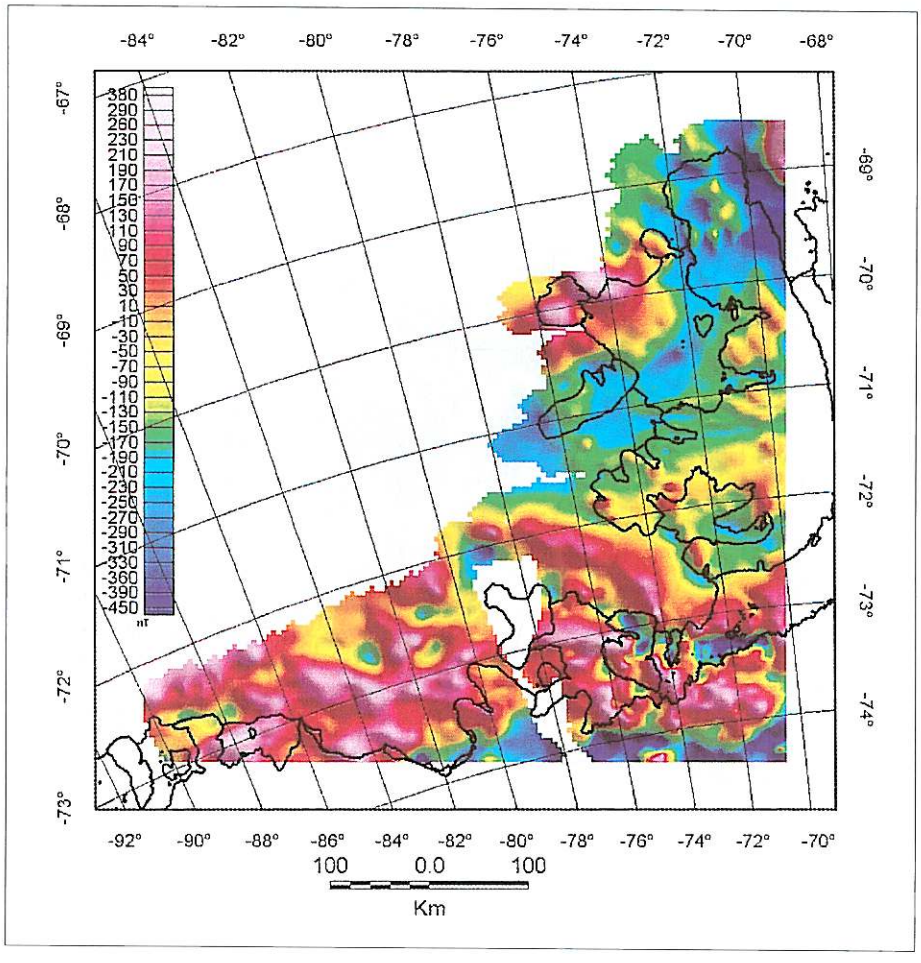

Fig. 2. Aeromagnetic anomaly map of reconnaissance data. Shading is from the northeast.

along the northern margin of Ellsworth Land, which have amplitudes up to 800 nT, is part of the Pacific Margin Anomaly (PMA). The PMA extends for some 2000 km along the Pacific margin of the Antarctic Peninsula and Ellsworth Land (Maslanyj *et al.*, 1991). The magnetic field over much of Alexander Island is typical of that seen over accretionary prisms (Johnson, 1996): a long wavelength, low amplitude background field punctuated by shorter-wavelength positive anomalies. A large (600 nT) positive anomaly is seen at the edge of the data, over Charcot Island (only two lines). Many of the western ends of the flight lines lie a considerable distance (up to 100 km) from the nearest tie line (fig. 1), which may give rise to levelling errors in those regions.

During the 1996-1997 Antarctic field season, an aeromagnetic survey was carried out by the BAS to the west of Alexander Island (fig. 1), designed to investigate the Charcot Island anomaly (Johnson and Ferris, 1997). Two wingtip-mounted Caesium-vapour magnetometers with a measurement accuracy of 0.01 nT were used.

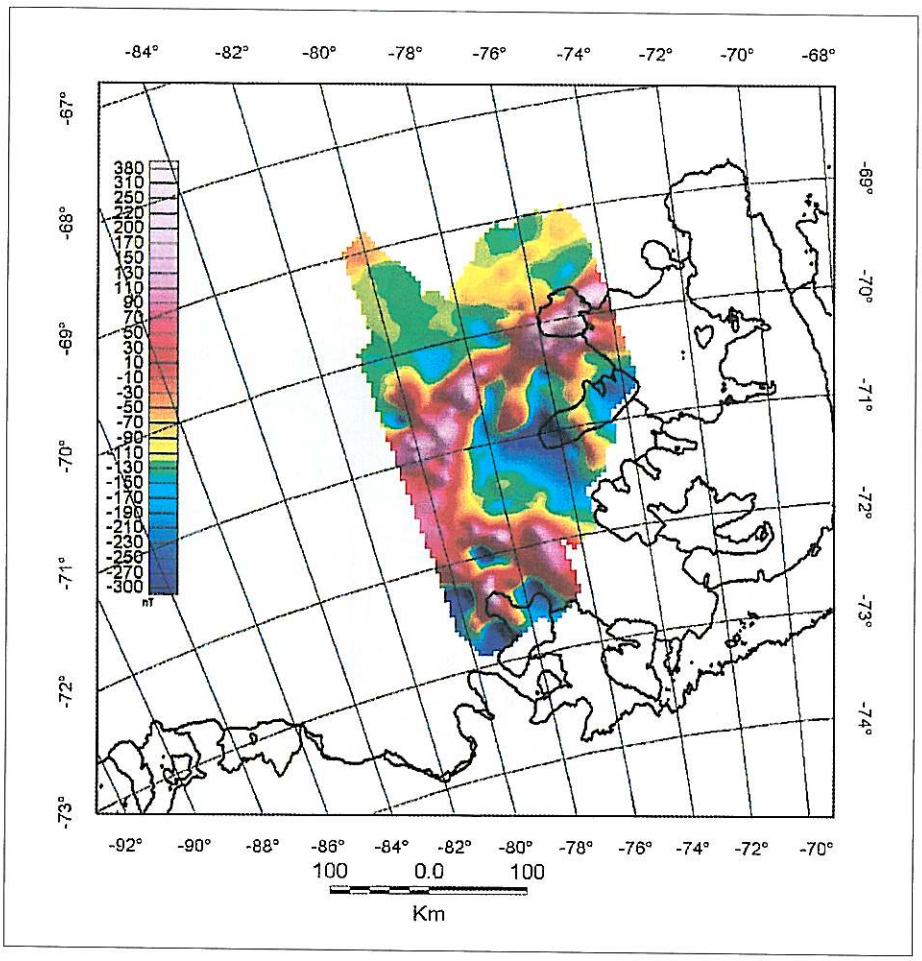

Fig. 3. Aeromagnetic anomaly map of Charcot survey data. Shading is from the northeast.

The magnetic effects of the aircraft were actively compensated using data from a triaxial fluxgate magnetometer mounted in the tail of the aircraft. Pseudorange GPS data were used for navigation, but dual-frequency continuous kinematic data were recorded which, when post-processed, gave positional accuracies of better than 5 m. Lines were flown at 10 or 20 km intervals (fig. 1). The flight height was generally 1000 m above m.s.l., though occasional departures from this height were necessary to clear topography, and to avoid icing conditions.

Processing of the data was carried out using the OASIS montaj™ Data Processing and Analysis system (Geosoft, 1997), which included data checking, merging navigation, continuation to a common elevation and removal of the 1995 IGRF (Barton, 1997).

The aeromagnetic map (fig. 3) shows the ENE-WSW linear trend of the Charcot anomaly, previously unknown from the reconnaissance data alone (compare fig. 2). The Charcot anomaly reaches an amplitude of 550 nT and appears to merge with the PMA at around 80°W. Anom-

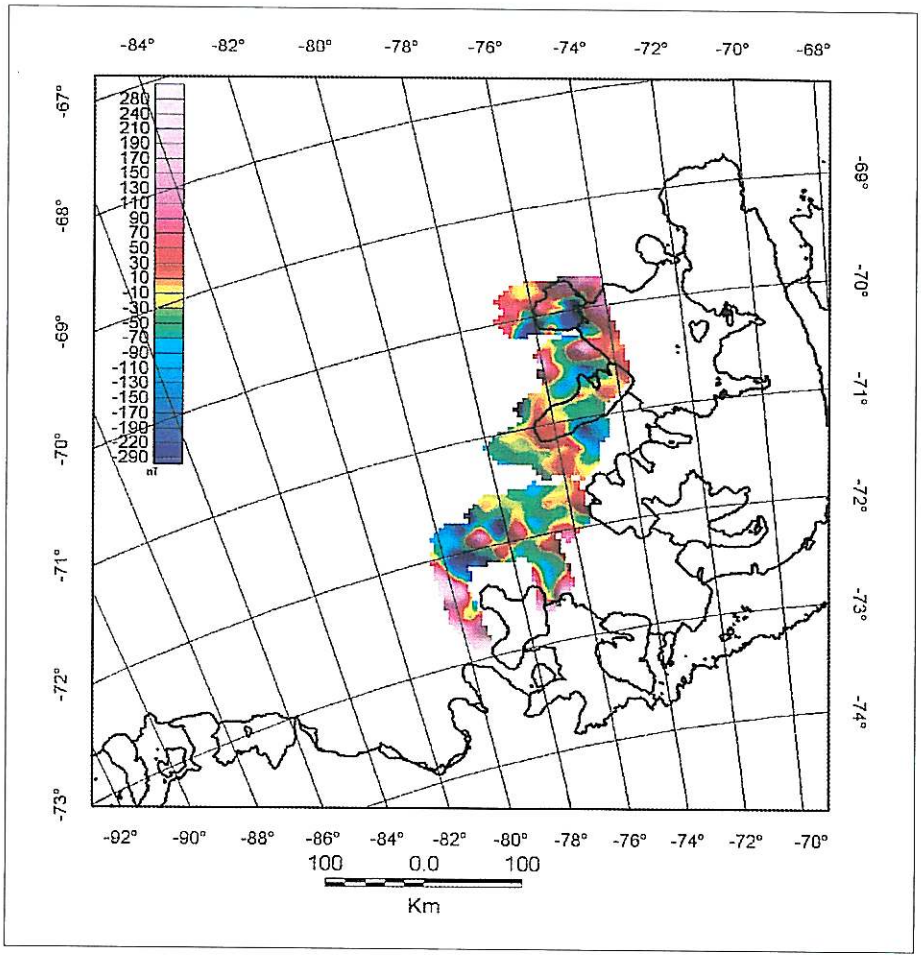

Fig. 4. Map of the difference between the reconnaissance (fig. 2) and Charcot data (fig. 3).

alies assumed to be part of the PMA can be seen in the Smyley Island area in the south of the map (fig. 3).

For the purposes of merging, both data sets were re-gridded at a 5 km interval. The Charcot grid was then upward-continued to a height of 2500 m above m.s.l. The two grids were subtracted from each other to examine the anomalies in the area of overlap (fig. 4). These differences range from – 400 to + 260 nT, many of which can be attributable to the different acquisition and processing parameters. Anomaly difference wavelengths vary from 10 to 50 km.

3. Grid merging techniques

The GridKnit™ system provides two advanced, rapid, interactive methods for merging grids, blending and suturing. The blending method is a well-established method, whereas the suturing method is both newly developed and newly implemented within the GridKnit™ system.

3.1. *Blending method*

This method uses a blending function over the area of overlap so that the transition from one grid to another is smooth. Except for the optional removal of a static offset or trend, the grids beyond the overlap regions remain unchanged.

The blending function determines the weighting of one grid against the other inside the overlap region. It works by calculating the minimum distance to the edge of each grid for each data point (fig. 5a). The function then uses a cosine taper (fig. 5b) which varies smoothly from 0 to 1, takes on a value of 0.5 at positions midway between two grids, and whose derivative approaches zero at both ends. If a position is equidistant between both edges, its value is the average of the grid values found at that point. The example in fig. 5b shows the value (on the cosine curve) for Grid 1 is around 0.7, and the value for Grid 2 is 0.3. This means that when the blending function calculates the value for that data point, it uses 0.7 of the value at the point on

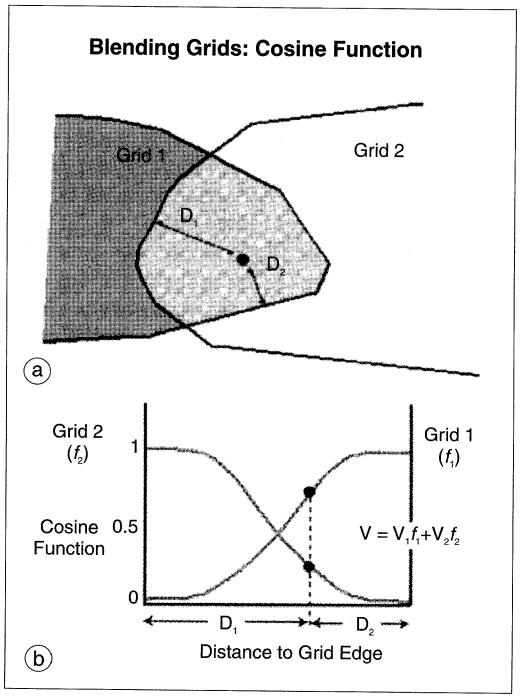

Fig. 5a,b. a) Schematic diagram showing overlap of two grids, Grid 1 and Grid 2. D_1 and D_2 are distances from a point in the overlap region to the edge of the overlap area; b) cosine taper function for grid blending scheme.

Grid 1 and 0.3 of the value at the point on Grid 2. Where the edges of Grid 1 and Grid 2 cross at a single point, the blending scheme breaks down, since by definition both grids are full owners of the point. In this case the average of the two values at the point is used.

3.2. *Suture method*

The suture method requires a line to be defined, at which to join the two grids. The line must lie completely within the overlapping area of the two grids. This suture line is used to truncate each grid and the cut-off sections of each grid have no contribution to the final grid. The GridKnit™ system can determine the suture line in a number of different ways: auto-

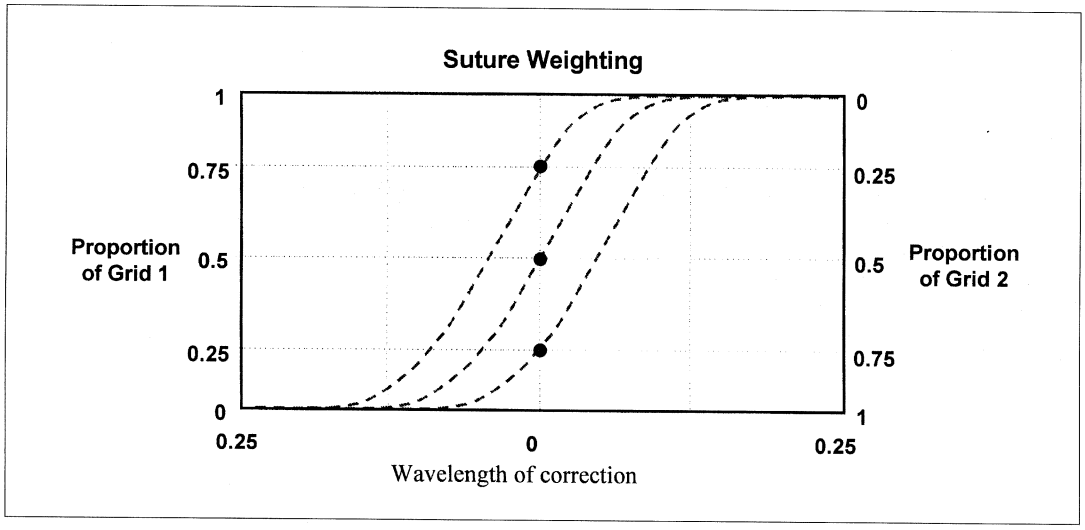

Fig. 6. Suture weighting. The numbers at the side of the chart represent the proportion of weighting for each grid. The horizontal axis represents the distance perpendicular to the suture line, which is proportional to the wavelength of each correction surface. The zero on the horizontal axis marks the suture line position.

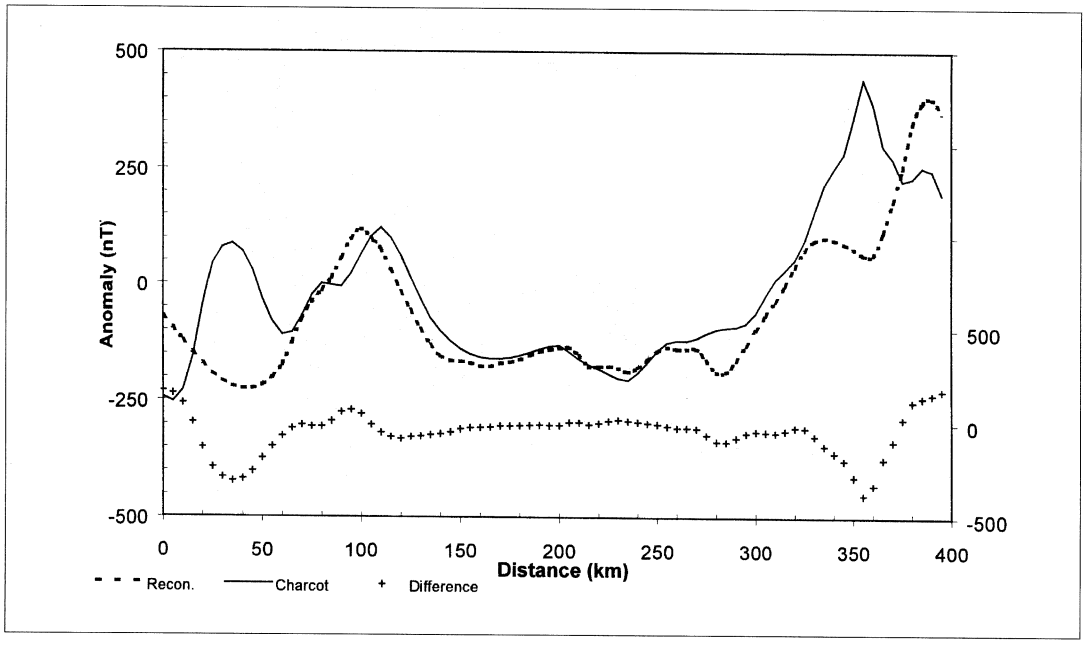

Fig. 7. Profile of data along suture line in overlap area of the BAS reconnaissance and Charcot grids. Lower line is the difference between the grids, with a separate scale on the right hand side.

matically bisecting the region of overlap, the edge of either grid, or digitised interactively. Along the suture line, a mismatch in the grid values is corrected by adjusting the grids on either side of the path. For instance, if for a point on the suture line the value for Grid 1 is larger than the value for Grid 2, then taking the average value could eliminate the discrepancy. Points adjacent to the line point might then be adjusted to produce a smooth transition between the two grids. The suture method uses a multi-frequency approach to spread corrections over the two grids in proportion to the wavelength of the mismatch found along the suture path. This ensures that the transition from one grid to the other remains smooth, whatever the amplitude and wavelength of the features that the suture path crosses.

A weighting coefficient in the range 0 to 1 determines how corrections are apportioned between the grids. A cosine function is used to weight the grids (fig. 6). For example, for the grid value (dot) closest to the bottom of fig. 6, the weighting function would use 0.25 of Grid 1

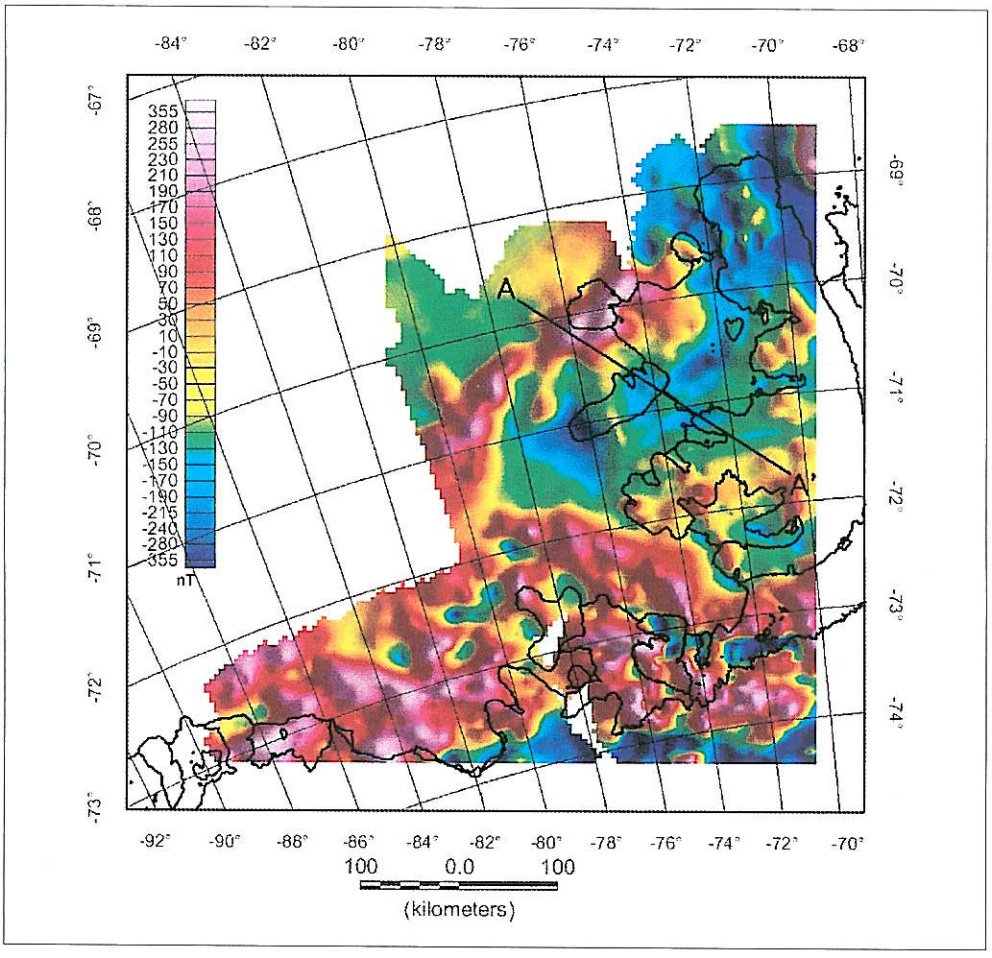

Fig. 8. Map of combined reconnaissance and Charcot grids, using the suture method. Line AA' indicates the position of the profile in figs. 9 and 10.

and 0.75 of Grid 2. Similarly, a value of 1 would mean that all corrections are applied to Grid 1. A value of 0 indicates that all corrections are applied to Grid 2, and value of 0.5 (dot in the centre of fig. 6) means corrections are shared equally between both grids. By default, the weighting is even between the grids, however, by forcing all the corrections toward one grid or the other, the user can keep one grid unaltered following the suture process, right up to the suture line.

To ensure that the suturing process creates the smoothest possible transition between grids, GridKnit™ uses a multi-frequency Fast Fourier Transform (FFT) function. The Fourier transform breaks a single, complex curve into a family of sine curves, each with a unique frequency and amplitude. GridKnit™ first selects the grid values along the suture line for each grid, then calculates the difference between the values of Grid 1 and Grid 2 (fig. 7).

The difference curve (fig. 7) is split using a Fourier transform function into many curves, each representing a unique frequency. A grid is then created for each of these curves. The grid extent either side the suture line is proportional to the frequency of the particular curve. This proportional correction means that short-wavelength features on a grid are given a short-wavelength correction and longer wavelength features are given a longer wavelength correction. The correction surface for each frequency is added to create an overall correction grid, which is then applied according to the correction weighting scheme (fig. 6) so that the grids join perfectly at the edges.

4. Application to Antarctic Peninsula data

Both the blending and the suture methods were applied to the reconnaissance and Charcot grids. The Charcot grid had no trend removed from it, and the reconnaissance grid was permitted to dc shift. For the suture method, the suture line was chosen as the edge of the Charcot grid in order to preserve the maximum amount of the more recent data. Figure 8 shows the resulting grid produced by the suture method. No obvious discontinuities exist at the edges of the overlap area. The merged data set (fig. 8) shows the continuity of the Charcot anomaly and the PMA

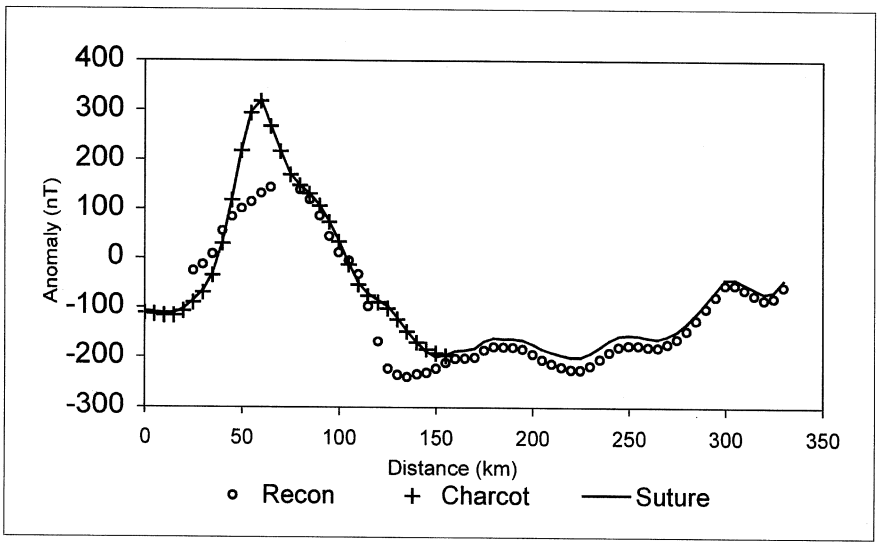

Fig. 9. Profiles extracted from the original (figs. 2 and 3) and sutured (fig. 8) grids. Position of profile is marked on fig. 8.

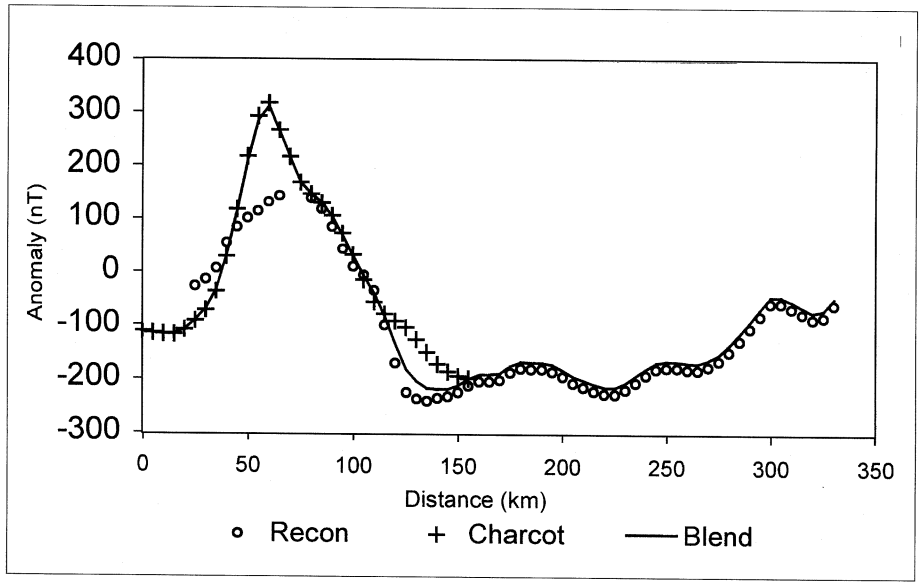

Fig. 10. Profiles extracted from the original (figs. 2 and 3) and blended (not shown) grids. Position of profile is marked on fig. 8.

between the two grids. Profiles (fig. 9) were extracted from the reconnaissance grid (fig. 2), the Charcot grid (fig. 3) and the sutured grid (fig. 8). The position of the profile is marked in fig. 8 (AA'). The profile (fig. 9) clearly shows the dc shift that has been applied to the BAS reconnaissance grid. The part of the profile across the overlap, about 30 km either side of the 100 km position (fig. 9), shows wavelengths on the suture profile similar to those in the original Charcot data ('+'s in fig. 9).

A profile in the same location was also extracted from the blended grid (grid not shown) and is shown in fig. 10. In the overlap region, it can be seen that the blending method has smoothed the anomalies to a greater extent than the suture method (fig. 9). Both methods have produced a smooth transition, and the results are very similar for this example. The wavelengths of anomalies remaining in the overlap region after merging are dependent on the suture line chosen. The suture method, however, appears to retain more of the appropriate wavelengths than the blending method.

5. Conclusions

Two grids of different age, with differing acquisition and processing parameters covering a remote area of the Bellingshausen Sea and Alexander Island, Antarctica have been merged into a single map for the first time. This merging was made considerably easier with a new interactive tool, GridKnit™. The two methods applied, blending and suturing, produce a smooth final result. The blending tool smoothes the overlap differences over the whole overlap area, whereas the suture tool applies corrections that are proportional to the wavelengths of the anomaly differences along a single suture line. Both techniques are rapid, and the implementation offers choice between full automation and complete user control. Tools exist for easy comparison and checking of results. The anomalies on the combined aeromagnetic map can now be interpreted in the wider context of the fore-arc of the Antarctic Peninsula, and the techniques applied to all the available data for the Antarctic as part of the ADMAP project.

REFERENCES

BARRACLOUGH, D.R. (1981): The 1980 International geomagnetic reference field, *Nature*, **294**, 14-15.

BARRACLOUGH, D.R. (1985): International geomagnetic reference field revision, *Nature*, **318**, 316.

BARTON, C.E. (1997): International geomagnetic reference field: the seventh generation, *J. Geomagn. Geoelectr.*, **49**, 123-148.

DODS, S.D., D.J. TESKEY and P.J. HOOD (1985): The new series of 1:1000000-scale magnetic-anomaly maps of the Geological Survey of Canada: Compilation techniques and interpretation, in *The Utility of Regional Gravity and Magnetic Anomaly Maps*, edited by W.J. HINZE, Society of Exploration Geophysicists, Tulsa, Oklahoma, 69-87.

FAIRHEAD, J.D., J.D. MISENER, C.M. GREEN, G. BAINBRIDGE and S.W. REFORD (1997): Large scale compilation of magnetic, gravity, radiometric and electromagnetic data: the new exploration strategy for the 90s, in *Proceedings of Exploration 97: Fourth Decennial International Conference on Mineral Exploration*, edited by A.G. GUBINS, GEO F/X, Canada, 805-816.

GEOSOFT (1997): *OASIS Montaj Data Processing and Analysis (DPA) System for Earth Science Applications, Version 4.1 user Guide*, Geosoft Inc., pp. 290.

JOHNSON, A.C. (1996): Arc evolution: a magnetic perspective from the Antarctic Peninsula, *Geol. Mag.*, **133**, 637-644.

JOHNSON, A.C. and J.K. FERRIS (1997): Reconnaissance aeromagnetic surveying of the Antarctic Peninsula margins using a Dash-7 aircraft, in *Proceedings of the Third International Remote Sensing Conference and Exhibition*, ERIM International Inc., Ann Arbor, MI, 685-692.

JOHNSON, A.C. and A.M. SMITH (1992): New aeromagnetic map of West Antarctica (Weddell Sea Sector): introduction to important features, in *Recent Progress in Antarctic Earth Science*, edited by Y. YOSHIDA, K. KAMINUMA and K. SHIRAISHI, Terrapub, Tokyo, 555-562.

JOHNSON, A.C., R.R.B. VON FRESE and THE ADMAP WORKING GROUP (1997): Magnetic Map Will Define Antarctica's Structure, *Eos, Trans. Am. Geophys. Un.*, **78**, 185.

MASLANYJ, M.P., S.W. GARRETT, A.C. JOHNSON, R.G.B. RENNER and A.M. SMITH (1991): *Aeromagnetic Anomaly Map of West Antarctica (Weddell Sea Sector)*, 1:2500000, British Antarctic Survey GEOMAP series Sheet 2, with supplementary text, British Antarctic Survey, Cambridge, pp. 32.

RENNER, R.G.B., L.J. STURGEON and S.W. GARRETT (1985): Reconnaissance gravity and aeromagnetic surveys of the Antarctic Peninsula, *Br. Antarc. Surv. Sci. Rep.*, **110**, 1-50.